



Article

Hepatocellular Carcinoma in Mice Affects Neuronal Activity and Glia Cells in the Suprachiasmatic Nucleus

Mona Yassine ¹, Soha A. Hassan ^{1,2,3} , Lea Aylin Yücel ¹, Fathima Faiba A. Purath ¹, Horst-Werner Korf ⁴ , Charlotte von Gall ^{1,*} and Amira A. H. Ali ^{1,5}

- ¹ Institute of Anatomy II, Medical Faculty, Heinrich Heine University, Moorenstraße 5, 40225 Düsseldorf, Germany; mona.yassine@hhu.de (M.Y.); soha.hassan@suezuniv.edu.eg (S.A.H.); leaaylin.yuecel@med.uni-duesseldorf.de (L.A.Y.); fathimafaiba.ambalapurath@med.uni-duesseldorf.de (F.F.A.P.); amira.ali@med.uni-duesseldorf.de (A.A.H.A.)
- ² Department of Zoology, Faculty of Science, Suez University, P.O. Box 43221, Suez 43533, Egypt
- ³ Department of Biology, University of Fribourg, 1700 Fribourg, Switzerland
- ⁴ Institute of Anatomy I, Medical Faculty, Heinrich Heine University, Moorenstraße 5, 40225 Düsseldorf, Germany; korf@uni-duesseldorf.de
- ⁵ Department of Human Anatomy and Embryology, Faculty of Medicine, Mansoura University, Mansoura 35516, Egypt
- * Correspondence: charlotte.gall@med.uni-duesseldorf.de; Tel.: +49-02118115044; Fax: +49-02118115046
- † These authors contributed equally to this work.

Abstract: Background: Chronic liver diseases such as hepatic tumors can affect the brain through the liver–brain axis, leading to neurotransmitter dysregulation and behavioral changes. Cancer patients suffer from fatigue, which can be associated with sleep disturbances. Sleep is regulated via two interlocked mechanisms: homeostatic regulation and the circadian system. In mammals, the hypothalamic suprachiasmatic nucleus (SCN) is the key component of the circadian system. It generates circadian rhythms in physiology and behavior and controls their entrainment to the surrounding light/dark cycle. Neuron–glia interactions are crucial for the functional integrity of the SCN. Under pathological conditions, oxidative stress can compromise these interactions and thus circadian timekeeping and entrainment. To date, little is known about the impact of peripheral pathologies such as hepatocellular carcinoma (HCC) on SCN. **Materials and Methods:** In this study, HCC was induced in adult male mice. The key neuropeptides (vasoactive intestinal peptide: VIP, arginine vasopressin: AVP), an essential component of the molecular clockwork (Bmal1), markers for activity of neurons (c-Fos), astrocytes (GFAP), microglia (IBA1), as well as oxidative stress (8-OHdG) in the SCN were analyzed by immunohistochemistry at four different time points in HCC-bearing compared to control mice. **Results:** The immunoreactions for VIP, Bmal1, GFAP, IBA1, and 8-OHdG were increased in HCC mice compared to control mice, especially during the activity phase. In contrast, c-Fos was decreased in HCC mice, especially during the late inactive phase. **Conclusions:** Our data suggest that HCC affects the circadian system at the level of SCN. This involves an alteration of neuropeptides, neuronal activity, Bmal1, activation of glia cells, and oxidative stress in the SCN.

Keywords: HCC; SCN; circadian system; VIP; AVP; glia; oxidative stress



Citation: Yassine, M.; Hassan, S.A.; Yücel, L.A.; Purath, F.F.A.; Korf, H.-W.; von Gall, C.; Ali, A.A.H. Hepatocellular Carcinoma in Mice Affects Neuronal Activity and Glia Cells in the Suprachiasmatic Nucleus. *Biomedicines* **2024**, *12*, 2202. <https://doi.org/10.3390/biomedicines12102202>

Academic Editors: Joanna Kamińska and Olga Koper-Lenkiewicz

Received: 29 August 2024

Revised: 21 September 2024

Accepted: 25 September 2024

Published: 27 September 2024



Copyright: © 2024 by the authors. Licensee MDPI, Basel, Switzerland. This article is an open access article distributed under the terms and conditions of the Creative Commons Attribution (CC BY) license (<https://creativecommons.org/licenses/by/4.0/>).

1. Introduction

Hepatocellular carcinoma (HCC) is the most common liver cancer worldwide and causes approximately one million deaths annually [1]. Recently, there has been an increasing number of HCC patients globally [2], often diagnosed at advanced stages after serious consequences have occurred due to the absence of specific symptoms and lack of diagnostic markers [3]. Non-specific symptoms of HCC include fatigue and sleep disturbance [4,5]. Generally, cancer-related fatigue (CRF) is caused by multiple central and peripheral factors, including neurotransmitter imbalance, systemic inflammation, and circadian disruption [6] that negatively impacts the patient's quality of life [5].

The hierarchically organized mammalian circadian system controls rhythms in behavior and physiology, such as activity, sleep, body temperature, hormone release, and food intake [7,8]. It contains a master circadian oscillator that generates an endogenous rhythm of approximately 24 h (circadian), input paths for the entrainment of the circadian rhythms with rhythmic external environmental cues, and output paths for the entrainment of subordinate oscillators. The master circadian oscillator resides in the hypothalamic suprachiasmatic nucleus (SCN) [9]. Rhythmic SCN activity is entrained to the light/dark cycle through the retino-hypothalamic tract (RHT). The integrated time information is transmitted via neuronal and endocrine connections to subordinate oscillators in the brain and the periphery. The SCN can be divided into two functionally different subregions: the ventrolateral core and the dorsomedial shell. Both regions use GABA as a transmitter but in combination with different neuropeptides, the vasoactive intestinal peptide (VIP) in the core region and arginine vasopressin (AVP) in the shell region [10]. The core is innervated by the RHT and innervates the shell, which in turn innervates other key regions of the hypothalamus [11]. At the cellular level, a molecular clockwork composed of transcriptional/translational feedback loops of clock genes controls rhythmic cell function. The transcription factor *Bmal1* is an essential component of molecular clockwork and is involved in the generation and entrainment of circadian rhythms in SCN [12,13]. At the SCN cellular network level, the coupling of both neurons and astrocytes [14,15], as well as VIP and AVP [10,16–19], contribute to both the stability and the entrainment of circadian rhythms. Light information is encoded by the release of glutamate and neuropeptides from RHT connecting to VIP neurons in the core. The stimulation of the respective receptors activates the MAPK/CRE-binding pathways and, subsequently, the neuronal activity marker *c-Fos* and clock gene *Per1* to reset the molecular clockwork [20–22].

So far, little is known about the pathomechanisms of structural and functional changes in the brain caused by chronic liver diseases. The liver–brain axis might involve visceral afferent connections, including sympathetic and parasympathetic nervous systems [23] and blood-borne signals such as immune cells, cytokines, and metabolites that reach the brain, particularly through a disease-related deficient blood–brain barrier [1,23,24]. In hepatic encephalopathy, ammonia and inflammation are the major triggers for oxidative stress, astrocytic/neuronal dysfunction, and subsequent disturbances of brain oscillatory networks [25–27]. HCC involves pathologies in liver structure and function associated with chronic inflammation, resulting in hepatocellular DNA damage, and can be recapitulated by the administration of genotoxic agents in animals [28]. HCC is associated with sleep–wake disturbance and poor sleep quality in patients [29]. Higher diurnal cortisol level suggests a disturbed circadian rhythm in HCC patients, which may underlie their poor sleep quality [30].

Clock genes are pivotal players that regulate cell proliferation and apoptosis in HCC [31]. Furthermore, they are considered potential diagnostic markers and therapeutic targets in HCC [32]. HCC affects transcription and posttranscriptional modification of clock genes [32] and, consequently, rhythmic functions also in other tissues [33–35], including the hippocampus [36].

In the hippocampus, HCC-dependent changes in clock genes are associated with upregulation of genes encoding for proinflammatory cytokines and reduced proliferation of neuronal progenitors [36], suggesting that liver cancer affects the molecular clockwork, the innate immune system, and adult neurogenesis in the brain. Moreover, we showed earlier that HCC is associated with changes in corticosterone rhythms, locomotor activity (reminiscent of fatigue), and pERK immunoreaction in SCN [37], suggesting that the circadian system is compromised by liver cancer. The aim of this study was to better understand the effect of HCC on the circadian system. We investigated the neuropeptides, SCN neuronal and glial activity, molecular clockwork, and oxidative stress in the context of HCC.

2. Materials and Methods

2.1. Animal Experiments and Tissue Preparation

The animal experiments were approved by the local authority, the Landesamt für Natur, Umwelt und Verbraucherschutz Nordrhein-Westfalen (Reference number: AZ 81-02.04.2018-A146) and were conducted according to Directive 2010/63/EU of European Parliament and the Council on the Protection of Animals Used for Scientific Purposes. The experimental design is described in detail in [35–37]. Briefly, 14-day-old male Per2::Luc mice with a C57BL6/J background were randomly divided into an experimental group and a control group. In the experimental group, HCC was chemically induced by a single intraperitoneal injection of the genotoxic agent diethylnitrosamine (10 mg/kg, Cat # N0756-10ML, Sigma Aldrich, Burlington, MA, USA). Phenobarbital (PB) was chronically added to the drinking water (0.05%, Luminal, Desitin, Hamburg, Germany) to enhance HCC development. The control group was only given PB in the drinking water (PB control). At the age of one month, mice were separated from their mothers, and litters were kept in groups of 3–4 mice per cage under 12 h light/12 h dark. During the light phase, the light intensity was 300 lx. Zeitgeber time (ZT) 00 is defined as the time when light was turned on (06:00 am), while ZT12 is defined as the time when light was turned off (06:00 pm). At the age of 7–8 months, mice were sacrificed at four different time points at six-hour intervals, starting at ZT02, thus two hours after lights were on (08:00 am), ZT08: eight hours after lights were on, ZT14: two hours after lights were off and ZT20: eight hours after the lights were off. This provides us with tissue collected at 2 different time points during the early and late light phase (ZT02, ZT08, respectively), and 2 different time points during the early and late dark phase (ZT14, ZT20) to allow the comparison between these time points and phases.

Mice were injected intraperitoneally with a mixture of ketamine (100 mg/kg, Actavis, Ireland) and xylazine (10 mg/kg, Bayer, Leverkusen, Germany), then were intracardially perfused with 0.9% NaCl, followed by 4% formalin, using a peristaltic pump (World Precision Instruments, Sarasota, FL, USA). For mice sacrificed during the dark phase, perfusion and tissue collection were performed exclusively under dim red light.

The livers were inspected for tumors (Figure S1). Of the experimental group, only the mice of comparable tumor size were included ($n = 12$), while animals with no visible or too small lesions were excluded ($n = 4$). Of the PB control group, all mice could be included because none had a tumor ($n = 12$). The brains were extracted, post-fixed in 4% formalin for additional 24 h, cryoprotected in 30% sucrose, and snap frozen. The brains were cryo-sectioned into series of free-floating 30 μm thick coronal sections. Series of sections, including the SCN from these animals, were used for immunohistochemical staining in our previous work [37], while the other series were used here to obtain our novel data published here.

2.2. Immunohistochemistry

All sections used for each marker were processed together at one staining set to avoid the variability in staining conditions.

2.2.1. Chromogenic Reaction

Step 1: Serial brain sections were washed with phosphate-buffered saline (PBS). Step 2: Sections were incubated with 0.6% H_2O_2 for 30 min, followed by washing with PBS containing 0.2% Triton (PBST). Step 3: Sections were incubated in PBST containing 5% normal goat serum (PBSTN) for one hour, followed by incubation with primary antibodies (Table 1) at 4 °C overnight. Step 4: The sections were incubated with the corresponding IgG-biotin-conjugated secondary antibody (Table 2) in PBSTN for one hour at room temperature. This was followed by washing with PBST and incubation with avidin/biotin-based peroxidase system (ABC kit, Vector Laboratories, Newark, CA, USA) for one hour. The sections were rinsed and, finally, incubated with 0.05% 3,3'-diaminobenzidine (DAB) for 5 min. Step 6:

Sections were rinsed with PBS, mounted on slides, and cover slipped using DePeX (Serva Electrophoresis, Heidelberg, Germany).

Table 1. Primary antibodies.

Antibody	Manufacturer	Concentration
Anti-VIP (rabbit, monoclonal, cat #4245)	BMA Biomedicals (Augst, Switzerland)	1:4000
Anti-AVP (rabbit, polyclonal, cat # AHP372)	BIO-RAD (Berkeley, CA, USA)	1:1000
Anti-Bmal1 (rabbit, monoclonal, cat #14268-1-AP)	Proteintech (Rosemont, IL, USA)	1:500
Anti-orexin (rabbit, monoclonal, cat # 16743)	Cells Signaling Technology (Danvers, MA, USA)	1:2000
Anti-IBA1 (rabbit, polyclonal, cat # 019-19741)	WAKO (Osaka, Japan)	1:2000
Anti-GFAP (mouse, monoclonal, cat # 556330)	BD Biosciences (Eysins, Switzerland)	1:500
Anti-8-OHdG (mouse, monoclonal, cat #AM03160PU-N)	ORIGENE (Herford, Germany)	1:1000
Anti-c-Fos (rabbit, monoclonal, cat #4384)	Cells Signaling Technology (Danvers, MA, USA)	1:1000

Table 2. Secondary antibodies.

Antibody	Manufacturer	Concentration
Anti-rabbit IgG Biotin (goat, cat # BA-1000)	Vector Laboratories (Burlingame, CA, USA)	1:500
Anti-rabbit IgG Alexa Fluor 488 (goat; cat # A-11036)	Molecular Probes (Eugene, OR, USA)	1:500
Anti-mouse IgG Alexa Fluor 568 (goat; cat # A-11031)	Molecular Probes (Eugene, OR, USA)	1:500

2.2.2. Immunofluorescence

The steps 1, 3, and 6 were performed as described in Section 2.2.1. Step 2 was omitted. Step 4 was performed as follows: sections were incubated with the corresponding IgG-AlexaFluor-conjugated secondary antibody (Table 2) diluted in PBST containing 5% normal goat serum for one hour at room temperature.

2.2.3. Antibody Specificity

The specificity of primary antibodies has been confirmed previously [38–44] and was also evident by cell morphology, subcellular localization, and region-specific distribution. The specificity of secondary antibody was confirmed by treating the sections as in Sections 2.2.1 and 2.2.2 described, but without adding primary antibody. To test the specificity of IgG-biotin-conjugated secondary antibody, sections were incubated with 0.6% H₂O₂ for 30 min and then in PBST containing 5% PBSTN at 4 °C overnight. The sections were incubated with IgG-biotin-conjugated secondary antibody in PBSTN for one hour at room temperature, followed by washing and incubation with avidin/biotin-based peroxidase system for one hour. The sections were rinsed and, finally, incubated with DAB for 5 min, then mounted on slides and cover slipped. To test the AlexaFluor-conjugated secondary antibody, the previous steps were repeated without incubation in 0.6% H₂O₂. The specificity was confirmed as a positive staining signal was not detected.

2.3. Image Acquisition and Analysis

Coronal sections containing the hypothalamus were imaged using $\times 20$ objective of a Keyence BZ-X800 microscope (Keyence, Osaka, Japan). During image acquisition and processing, all settings, including illumination intensity and step size, were kept constant for each staining set. The analysis was performed by an investigator blind to the experimental conditions. Image analysis was performed using ImageJ (Version 1.53a) software [45]. This automated analysis helps obtain standardized and accurate quantification of staining. The SCN was demarcated in the coronal brain sections due to the presence of densely packed nuclei dorsal to the optic chiasm on both sides of the lateral ventricle in the hypothalamic area from Bregma -0.34 to -0.7 [46]. Boundaries were traced using ImageJ's freehand tool (Figure S2A). The immunoreactions were analyzed in the middle part of the rostrocaudal extent in the right and left SCN from 1 to 2 sections per mouse and then averaged to obtain one value per animal. The intensity of background signal in the adjacent neuropil was subtracted from the respective intensity of immunostaining for VIP, AVP, Bmal1, glial fibrillary acidic protein (GFAP), IBA1, and 8-hydroxydeoxyguanosine (8-OHdG) in the SCN, and the resulting intensity was given in arbitrary units (A.U.). The number of c-Fos-immunoreactive cells in the delineated SCN area was counted and given in cells/mm². The lateral hypothalamus was demarcated in the coronal brain sections due to the presence of orexin-immunoreactive neurons in the area from Bregma -1.22 to -2.18 [46]. Boundaries were traced using ImageJ's freehand tool (Figure S2B). The number of orexin-immunoreactive cells in the delineated area of the lateral hypothalamus was counted and given in cells/mm².

2.4. Statistical Analysis

GraphPad Prism 8 software was used for statistical analysis. Data are expressed as mean \pm standard error of the mean (SEM). Two-way analysis of variance (ANOVA) was used to examine the effect of time and HCC and their interaction, followed by Sidak's multiple comparisons test. The results were regarded as significant when p value was <0.05 .

3. Results

3.1. Effect of HCC on Neuropeptides in SCN and Lateral Hypothalamus

VIP is expressed by neurons in the SCN core region and is crucial for synchronization of the neuronal network within the SCN [10]. VIP-immunoreactive neurons were found in the SCN of both groups (Figure 1A–H). Their cell bodies were found primarily in the core region, while their axons extended into the shell region (Figure S3A–C). Two-way ANOVA showed an effect of HCC ($F(3,16) = 12.3$, $p = 0.003$). Post hoc multiple comparisons showed a significantly higher intensity of VIP-immunoreaction (IR) in HCC mice than in PB controls in the late dark/activity phase (ZT20, $p = 0.04$) (Figure 1D,H,I).

AVP is also a synchronizer for SCN neurons and plays an important role in determining the period length and the anticipatory behavior [10]. AVP-immunoreactive neurons and axons were found in SCN of both groups, mainly in the shell regions (Figures 2A–H and S3D,E). Two-way ANOVA showed an effect of HCC ($F(3,16) = 18.7$, $p = 0.0005$) ($F(3,16) = 0.5$, $p = 0.66$). Post hoc multiple comparisons showed a significantly higher intensity of AVP-IR in HCC mice than in PB controls in the late dark/activity phase (ZT20, $p = 0.03$) (Figure 2D,H,I).

Orexin-immunoreactive neurons in the lateral hypothalamus play an essential role in the control of the sleep–wake cycle and the locomotor activity downstream of SCN. Two-way ANOVA showed no effect of HCC ($F(3,16) = 0.7$, $p = 0.59$) on the number of orexin-immunoreactive neurons in the lateral hypothalamus (Figure 3A–I).

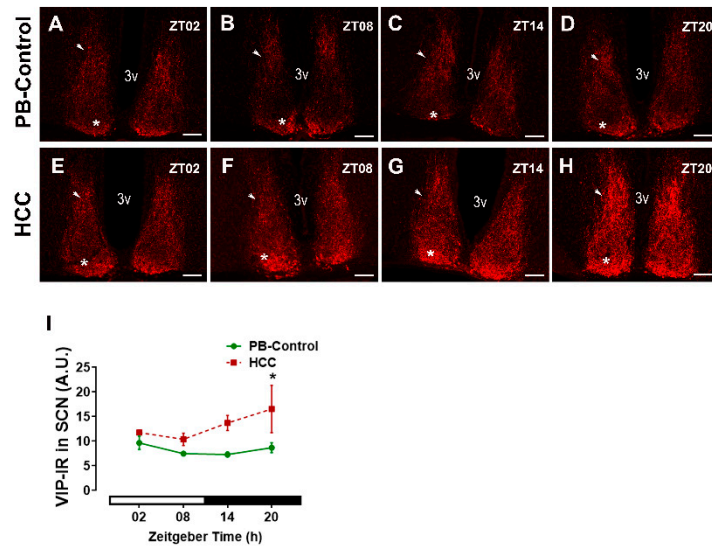


Figure 1. Vasoactive intestinal peptide (VIP) immunoreaction (IR) in the SCN. Representative fluorescent microphotographs showing the immunoreaction (IR) of VIP (red) in the suprachiasmatic nucleus (SCN) of (A–D) PB control mice and (E–H) HCC mice. The white asterisk indicates the ventral core region, while white arrowhead indicates the dorsal shell region of SCN. 3v: third ventricle. Scale bar = 100 μ m. Mice were sacrificed at different time points at 6 h intervals starting at Zeitgeber time (ZT) 02 = 2 h after the light on. (I) Quantification of VIP-immunoreaction (IR) in arbitrary unit (A.U.) in the SCN. White and black bar indicates light/dark phase, respectively. Two-way ANOVA followed by Sidak’s multiple comparisons test. Total of 12 mice per group, n = 3 mice at each time point. *: $p < 0.05$ between PB control and HCC.

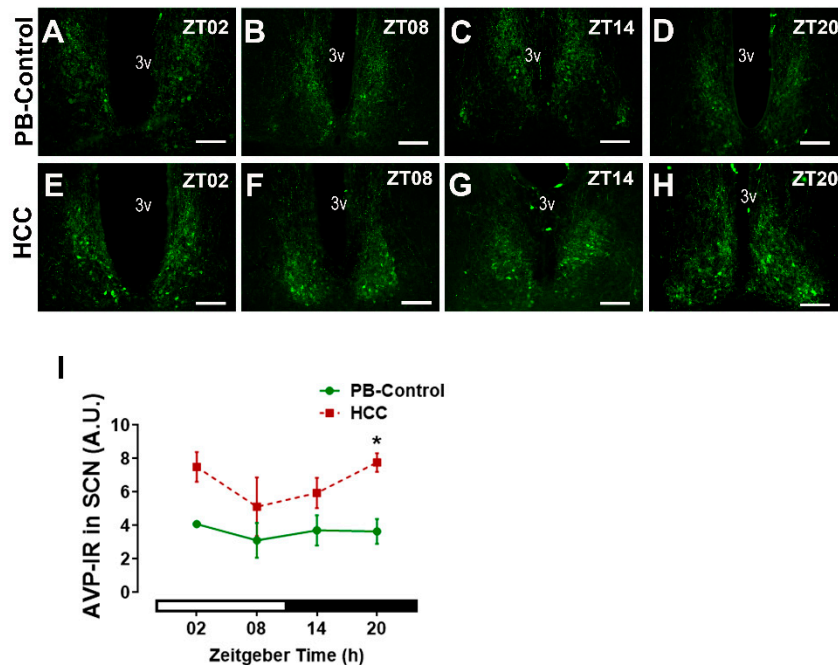


Figure 2. Arginine vasopressin (AVP) immunoreaction (IR) in the SCN. Representative fluorescent microphotographs showing the immunoreaction (IR) of AVP (green) in the SCN of (A–D) PB control mice and (E–H) HCC mice. 3v: third ventricle. Scale bar = 100 μ m. Mice were sacrificed at different time points at 6 h intervals starting at ZT02 = 2 h after the light was on. (I) Quantification of AVP-immunoreaction (IR) in arbitrary unit (A.U.) in the SCN. White and black bar indicates light/dark phase, respectively. Two-way ANOVA followed by Sidak’s multiple comparisons test. Total of 12 mice per group, n = 3 mice at each time point. *: $p < 0.05$ between PB control and HCC.

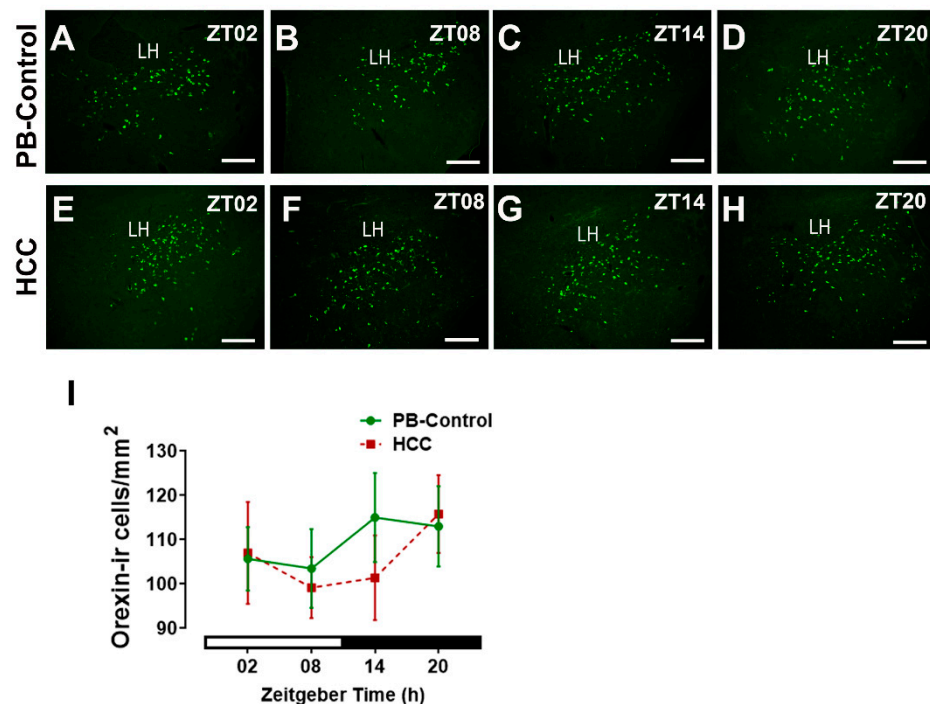


Figure 3. Orexin-immunoreactive (ir) cells in the lateral hypothalamus. Representative fluorescent microphotographs showing orexin-ir cells (green) in the lateral hypothalamus (LH) of (A–D) PB control mice and (E–H) HCC-bearing mice. Scale bar = 200 μ m. Mice were sacrificed at different time points at 6 h intervals starting at ZT02 = 2 h after the light was on. (I) Quantification of number of orexin-immunoreactive cells per mm^2 in the lateral hypothalamus. White and black bar indicates light/dark phase, respectively. Two-way ANOVA followed by Sidak’s multiple comparisons test. Total of 12 mice per group, $n = 3$ mice at each time point.

3.2. Effect of HCC on Bmal1-Immunoreactive Cells in SCN

Immunoreactive cells for the essential circadian clock protein Bmal1 (Figure 4A–H) showed no differences in the distribution between the two SCN subregions. Two-way ANOVA showed an effect of HCC ($F(3,16) = 13.7, p = 0.002$) ($F(3,16) = 2.0, p = 0.16$). Post hoc multiple comparisons showed a significantly higher intensity of Bmal1-IR in HCC mice than in PB controls in the late dark/activity phase (ZT20, $p = 0.006$) (Figure 4D,H,I).

3.3. Effect of HCC on the Neuronal Activity Marker c-Fos in SCN

The immunoreaction of c-Fos, the neuronal activity marker, was found in SCN cells of both groups (Figure 5A–H). Two-way ANOVA showed an interaction between time of day and HCC ($F(3,16) = 5.2, p = 0.02$). Post hoc multiple comparisons showed a significantly lower number of cFos-immunoreactive cells in HCC mice than in PB controls in the late light/inactive phase (ZT08, $p = 0.04$) (Figure 5B,E,I).

3.4. Effect of HCC on Astrocytic Marker GFAP in SCN

To investigate if HCC affects astrocytes in the SCN, we used the marker of astrocytic processes GFAP, whose increase within brain tissue indicates reactive astrocytes [47] (Figure 6A–H). Two-way ANOVA showed an effect of HCC ($F(3,16) = 19.6, p = 0.0004$). Post hoc multiple comparisons showed a significantly higher intensity of GFAP-IR in HCC mice than in PB controls in the late dark/active phase (ZT20, $p = 0.003$) (Figure 6D,H,I).

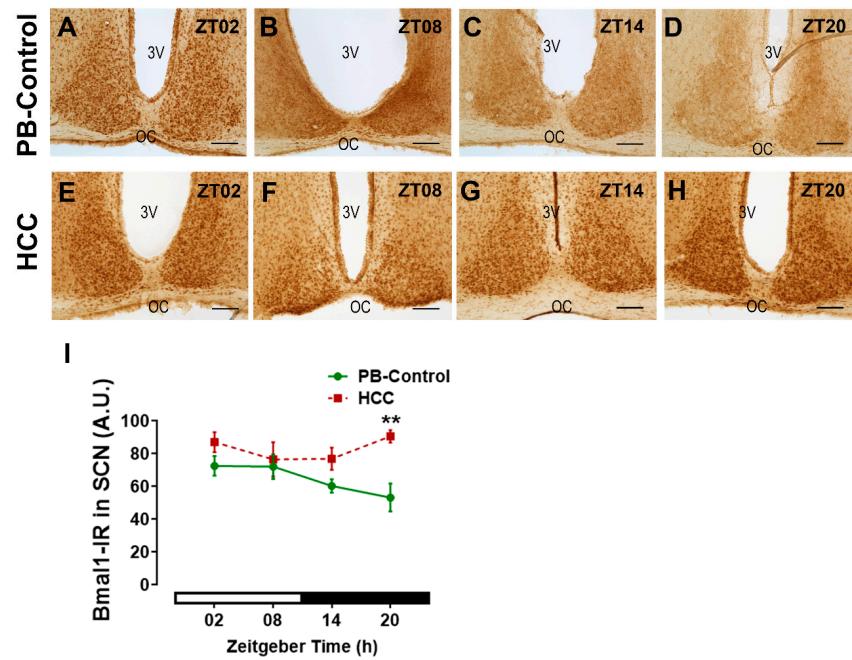


Figure 4. Bmal1-immunoreaction (IR) in the SCN. Representative bright-field photomicrographs showing the Bmal1-immunoreactive cells (brown staining) in the SCN of (A–D) PB control mice and (E–H) in HCC-bearing mice. 3v: third ventricle. OC: optic chiasma. Scale bar = 100 μ m. Mice were sacrificed at different time points at 6 h intervals starting at ZT02 = 2 h after the light on. (I) Quantification of Bmal1-IR in arbitrary units (A.U.) in the SCN at individual time points at 6 h intervals. White and black bar indicates light/dark phase, respectively. Two-way ANOVA followed by Sidak’s multiple comparisons test. Total of 12 mice per group, n = 3 mice at each time point. **: $p < 0.01$ between PB control and HCC.

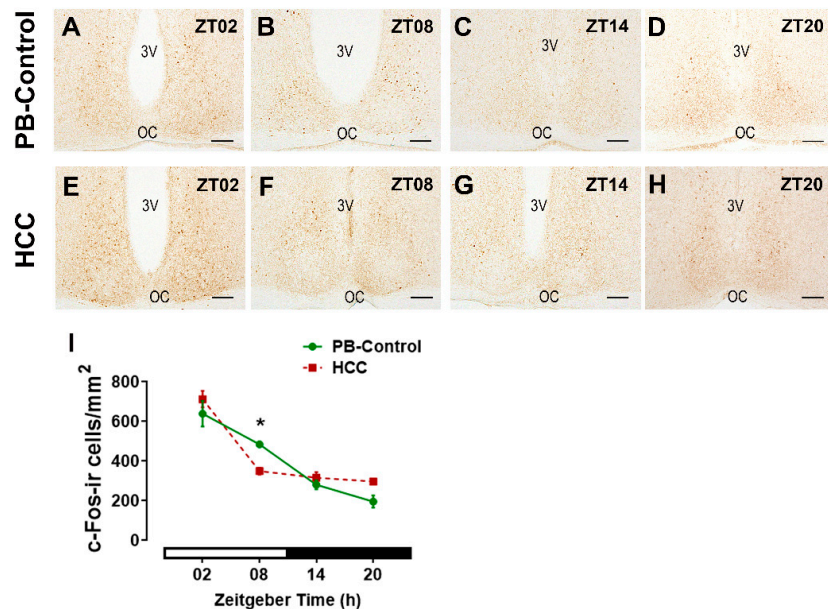


Figure 5. c-Fos-immunoreactive (ir) cells in the SCN. Representative bright-field photomicrograph showing the positively stained c-Fos cells (brown staining) in the SCN of (A–D) PB control mice and (E–H) in HCC-bearing mice. 3v: third ventricle. OC: optic chiasma. Scale bar = 100 μ m. Mice were sacrificed at different time points at 6 h intervals starting at ZT02 = 2 h after the light was on. (I) Quantification of c-Fos-ir cells/mm² in the SCN. White and black bar indicates for light/dark phase, respectively. Two-way ANOVA followed by Sidak’s multiple comparisons test. Total of 12 mice per group, n = 3 mice at each time point. *: $p < 0.05$ between PB control and HCC.

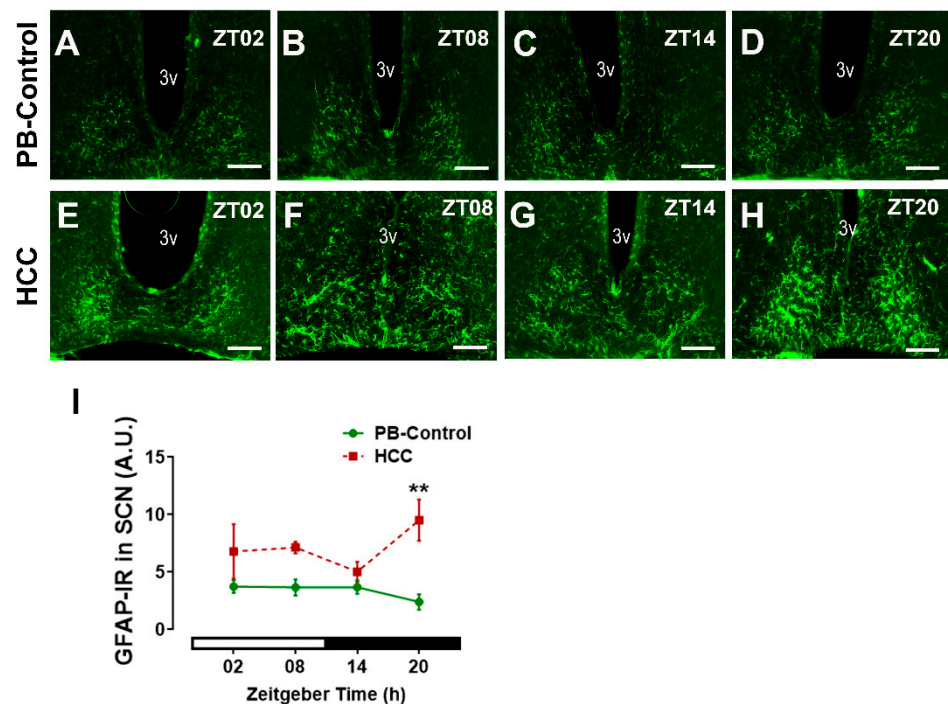


Figure 6. Astrocytic marker GFAP-immunoreaction (IR) in SCN. Representative fluorescent microphotographs showing GFAP immunoreaction (IR) (green) in the SCN of (A–D) PB control mice and (E–H) HCC mice. 3v: third ventricle. Scale bar = 150 μ m. Mice were sacrificed at different time points at 6 h intervals starting at ZT02 = 2 h after the light was on. (I) Quantification of GFAP-immunoreaction (IR) in arbitrary unit (A.U.) in the SCN. White and black bar indicates light/dark phase, respectively. Two-way ANOVA followed by Sidak’s multiple comparisons test. Total of 12 mice per group $n = 3$ mice at each time point. **: $p < 0.01$ between PB control and HCC.

3.5. Effect of HCC on Microglial Marker IBA-1 in SCN

We analyzed whether HCC induced microglial activation in SCN as an inflammatory response by use of IBA-1, the most commonly used marker for microglia [48]. IBA-1-immunoreactive microglia were detected in the SCN of PB control mice (Figure 7A–D) and the HCC-bearing mice (Figure 7E–H). Two-way ANOVA showed an effect of HCC ($F(3,16) = 16.2$, $p = 0.001$). Post hoc multiple comparisons showed a significantly higher intensity of IBA1-IR in HCC mice than in PB controls in the late dark/active phase (ZT20, $p = 0.002$) (Figure 7D,H,I).

3.6. Effect of HCC on Oxidative Stress Marker 8-OHdG in SCN

To analyze whether HCC induced oxidative stress in SCN, we investigated the DNA oxidative stress marker 8-hydroxydeoxyguanosine (8-OHdG) (Figure 8A–H). Two-way ANOVA showed an effect of HCC ($F(3,16) = 21.7$, $p = 0.0003$). Post hoc multiple comparisons showed a significantly higher intensity of 8-OHdG-IR in HCC mice than in PB controls in the early light/inactive phase (ZT02, $p = 0.03$) (Figure 8A,E,I) and early dark/active phase (ZT14, $p = 0.04$) (Figure 8C,G,I).

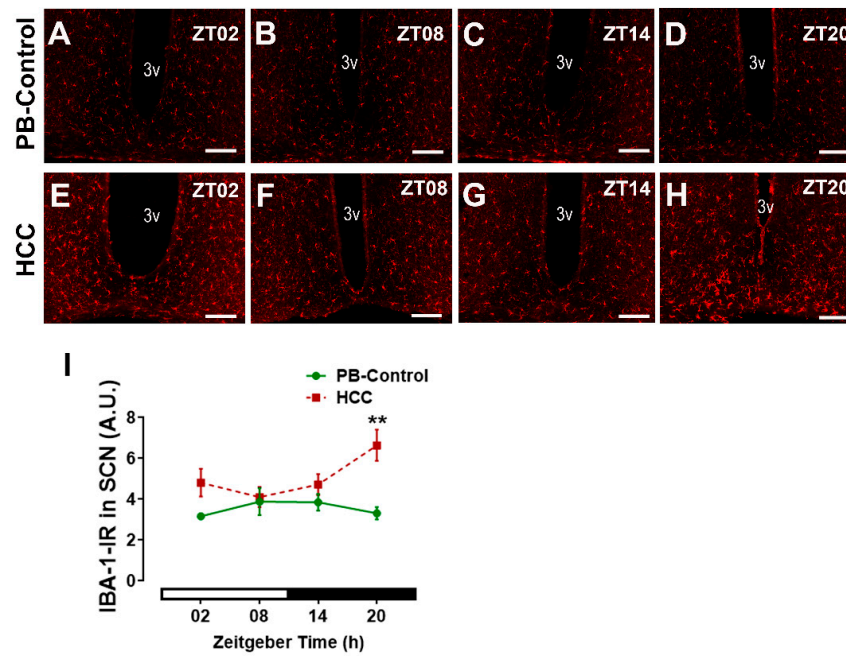


Figure 7. Microglial marker IBA-1-immunoreaction (IR) in SCN. Representative fluorescent photomicrographs showing IBA-1-immunoreaction (IR) (red) in the SCN of (A–D) PB control mice and of (E–H) HCC-bearing mice. 3v: third ventricle. Scale bar = 150 μ m. Mice were sacrificed at different time points at 6 h intervals starting at ZT02 = 2 h after the light was on. (I) Quantification of IBA-1-immunoreaction (IR) in arbitrary unit (A.U.) in the SCN. White and black bar indicates for light/dark phase, respectively. Two-way ANOVA followed by Sidak’s multiple comparisons test. Total of 12 mice per group, n = 3 mice at each time point. **: $p < 0.01$ between control and HCC.

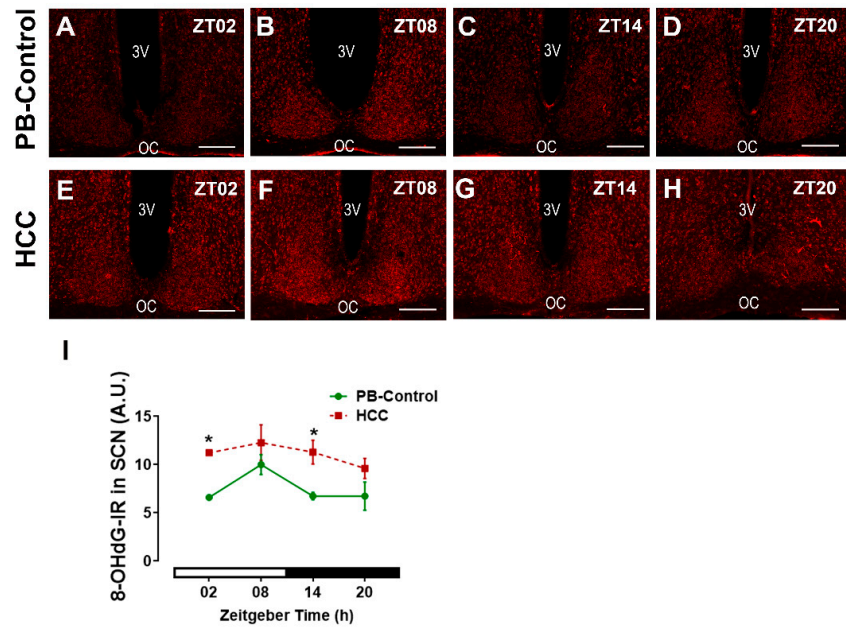


Figure 8. Oxidative stress marker 8-OHdG-immunoreaction (IR) in SCN. Representative fluorescent photomicrographs showing the immunoreaction (IR) of 8- hydroxydeoxyguanosine (8-OHdG) (red) in the SCN of (A–D) PB control mice and of (E–H) HCC-bearing mice. 3v: third ventricle. OC: optic chiasma. Scale bar = 100 μ m. Mice were sacrificed at different time points at 6 h intervals starting at ZT02 = 2 h after the light was on. (I) Quantification of 8-OHdG-immunoreaction (IR) in arbitrary unit (A.U.) in the SCN. White and black bar indicates light/dark phase, respectively. Two-way ANOVA followed by Sidak’s multiple comparisons test. Total of 12 mice per group, n = 3 mice at each time point. *: $p < 0.05$ between PB control and HCC.

4. Discussion

There is increasing evidence of a bidirectional relationship between cancer and the circadian system. On the one hand, cancer patients suffer from sleep–wake disturbances and decreased activity, known as cancer-related fatigue [1]. On the other hand, circadian disruption is a potential risk factor for the development and progression of some cancers, including malignant breast and gastrointestinal tumors [49].

In this study, we provide novel evidence that HCC in mice leads to significant changes at the level of the key component of the circadian system, the SCN. In particular, we see changes in neuropeptides and the activity of neurons and glial cells, as well as increased oxidative stress in SCN.

We previously showed a significant reduction in the overall locomotor activity, especially during the dark phase, reduced the amplitude of the activity rhythm, and reduced the neuronal activity in SCN during the light phase [37]. In accordance, mice with chemically induced HCC showed alterations in the locomotor activity rhythm [50]. These tumor-related changes in mice are similar to the symptoms of patients with ovarian, breast, liver, and colorectal tumors [51,52], indicating an effect of tumorigenesis on the circadian system, such as reduced activity, increased fatigability, and activity–sleep rhythm abnormalities. Furthermore, the SCN becomes less sensitive to the environmental photic cues in patients with liver cirrhosis [53], which is considered a premalignant condition [54]. Thus, HCC mice and patients with malignant tumors seem to share common changes in the circadian system. On the one hand, the SCN clockwork ensures the anticipation of the light and dark phases. On the other hand, the SCN clockwork is adaptively modulated by the light/dark information through a projection from the retina.

In SCN, neuropeptides, particularly VIP and AVP, are important for synchronization with the light/dark cycle to sculpt critical features of the sleep–wake cycle and for determining the period of circadian rhythms [10,17,18,55–57]. Both VIP- and AVP-immunoreactive SCN neurons play an important role in mediating the circadian output rhythm to subordinate oscillators in the brain, such as the paraventricular nucleus of the hypothalamus (PVN) which controls rhythms in the autonomic nerve system [58], secretion of hormones such as melatonin [58], and glucocorticoids [10] as well as the sleep–wake cycle [10]. These appear to be species-dependent differences in whether the AVP- and VIP-immunoreaction exhibit a time-of-day-dependent rhythm [59–61]. However, there is no question that the VIP+ neurons in the mouse SCN are activated by light and play an essential role in light entrainment of locomotor activity rhythm [17,18]. Importantly, both the VIP- and the AVP-IR are higher in the SCN of HCC mice than in the PB control mice. This is consistent with VIP and its VPAC receptors being upregulated in various tumors, including HCC [62], pancreas [63], lung [51], breast cancers [64], and glioma [65]. This upregulation is probably due to inflammatory processes associated with cancer development [62]. Although we cannot conclude from immunohistochemistry whether the higher staining intensity of neuropeptides reflects higher or lower secretory activity, a change in staining intensity definitely reflects a change in functional status.

We could show earlier that in the brains of HCC mice, the expression of genes encoding for proinflammatory cytokines is increased [36], supporting this hypothesis. Moreover, we could show earlier that the serum corticosterone levels are increased in HCC mice [37]. However, we cannot differentiate whether this is due to the inflammatory response or the disruption of the output of the SCN to the PVN or the hypothalamic–pituitary–adrenal (HPA) axis. Nevertheless, glucocorticoids not only provide time information for peripheral clocks but also modulate the VIP and AVP systems in the SCN [66]. Thus, increased immunoreaction of VIP and AVP in the SCN of HCC mice observed in this study might be due to the inflammatory response mediated by cytokines and/or glucocorticoids. In addition, metabolic changes associated with HCC can have a neuroactive effect (also see below).

Orexin is a neuropeptide exclusively produced by a specific subset of neurons in the lateral hypothalamus, and its dysfunction is associated with increased sleepiness

and decreased activity [67,68]. Since there was no effect of HCC on orexin-IR in the lateral hypothalamus, a general impact on neuropeptide expression throughout the brain is unlikely.

VIP is important for robust rhythms in clock gene expression in the SCN and some peripheral organs [69] and for the entrainment of circadian rhythms to the light/dark cycle [10,18], presumably through CRE activation in the SCN [70], leading to c-Fos and clock gene expression [71]. However, chemogenetic activation of VIP+ SCN neurons attenuates the amplitude of circadian rhythms in the SCN, consistent with the concept that high levels of VIP lead to reduced synchronization between SCN cells [72]. Thus, the alteration of VIP and AVP systems in the SCN of HCC mice observed in this study might contribute to reduced precision in the alignment of activity to the light/dark cycle and the decreased amplitude in their activity rhythm previously reported in [37]. Consistently, the higher VIP-IR in HCC mice was associated with a decrease in c-Fos-IR (this study), similar to the decrease in pERK-IR [37] and an increase in Bmal1-IR (this study).

Bmal1 is essential for circadian rhythm generation [73] and the robustness of rhythmic activity in the light/dark cycle [12]. In addition, Bmal1 is involved in the light-induced resetting of the SCN [13]. Bmal1-IR in the SCN shows no fluctuation depending on the time of day and is not affected by light [74]. Consistently, there was no effect of time on Bmal1-IR in the SCN of both groups. However, Bmal1 plays a critical role in circadian misalignment [75], and overexpression of Bmal1 leads to damping of SCN circadian rhythms [76]. Bmal1-IR was higher in the SCN of HCC mice compared to PB controls, suggesting a circadian misalignment and a mild overexpression. Thus, the lower levels of c-Fos and the higher levels of Bmal1 in the SCN of HCC mice might be due to the changes in the secretory activity of VIP+ neurons and might contribute to the reduced precision in the alignment of the activity rhythm to the light/dark cycle. Importantly, c-Fos is expressed in neurons only, while Bmal1 is also expressed in glia cells [14]. SCN astrocytes are important components of the rhythm-generating network, e.g., by regulating the balance between VIP and GABA [77]. They can initiate and maintain robust circadian activity rhythms and determine the circadian period [14,78]. Bmal1 might be involved in the regulation of the fine astrocytic processes that contribute to the chemical synapse [79]. The increased GFAP-IR in HCC mice indicates activation of astrocytes associated with the downregulation of their supportive function and upregulation of their proinflammatory function [80]. This might contribute to the alteration of neurotransmitter balance, reduced robustness of rhythmic locomotor activity, and also affect neurotransmission. Although there is no evidence for the involvement of microglia in the SCN circadian clock under physiological conditions [81], activation of proinflammatory microglia in SCN is associated with reduced rhythm amplitude in SCN slices [82]. The increased IBA-IR in HCC mice indicates activation of microglia accompanied by upregulation of their proinflammatory activity [83], which may contribute to impaired SCN function. Similarly, other peripheral malignant tumors, including breast cancer, trigger neuroinflammation and activation of glia cells [1,84] to secrete neurotoxic factors and chemokines and promote the recruitment of immune cells across the blood–brain barrier [80]. We hypothesize that cancer-related fatigue is related to impaired SCN function. Activation of astrocytes and microglia associated with liver diseases is also consistent with previous studies and may be a homeostatic response to protect brain tissue from higher levels of circulating cytokines and/or neuroactive/-toxic metabolites such as ammonia [85–88]. Both activated astrocytes and microglia can contribute to oxidative stress [89–91]. The increased IR for 8-OHdG-IR, a marker of DNA and RNA oxidative damage, in HCC mice, is consistent with higher oxidative/nitrosative stress and neuroinflammation in liver diseases [25,92,93]. Oxidation of DNA and RNA might contribute to transcriptional and posttranscriptional modulation of clock gene expression in the SCN of HCC mice [32]. This mechanism might be related to the effect of melatonin, which can act as a scavenger for radical oxygen species, on the consolidation of rhythmic locomotor activity in HCC mice [50]. In addition, our previous findings revealed that HCC triggered an increase and disruption in the rhythmic glucocorticoid in mice [37]. Similar

results were observed in HCC [30] and metastatic colorectal patients [94]. This chronic increase in glucocorticoids stimulates the stress response pathway via the HPA axis, which in turn stimulates the immune system to secrete various cytokines and chemokines, leading to neuroinflammation [95].

However, in the hippocampus of HCC mice, the expression of inflammatory cytokines and clock genes was increased, and the number of proliferating cells in the neurogenic niche was decreased, while the IR for c-Fos, pERK, GFAP, IBA, and 8-OHdG was not affected [36,37]. This suggests a brain region-specific difference in the response of neurons and glia cells to HCC and a modulation of clock gene transcription and adult neurogenesis by tumor-associated factors independent of oxidative stress.

Importantly, dysregulation of the endogenous circadian clock due to consuming alcohol, high-fat diets, shift work, or jet lag misaligns the liver's rhythmic metabolism and, thus, leads to liver pathologies such as HCC. A mice model with circadian malfunction due to chronic jet lag revealed more tendency to develop HCC in non-alcoholic fatty liver disease (NAFLD) due to disruption of the cell cycle components, including cell proliferation and apoptosis, and activation of oncogenic pathways such as WNT/ β -catenin and TNF α -NF- κ B in the liver [96].

This study has some limitations. The semi-quantitative measurements of the immunoreaction of relevant markers for neuronal and glial activity in the SCN have some limitations. While immunohistochemistry has the great advantage that it is restricted to the specific area under investigation and the signal is not "contaminated" by other brain areas as is the case in biochemical analyses of punch preparations, it cannot be determined whether the higher staining intensity of neuropeptides reflects higher secretory activity or storage of neuropeptides. This question can be solved only by additional invasive procedures such as microdialysis in future studies. It has been shown that HCC is more prevalent in males [97]; however, circadian rhythms are disrupted in both male and female HCC patients [30]. In addition, there is a sex-specific effect in a wide variety of circadian functions as well as in the response to chronodisruption [98]. Thus, it is still important to include HCC-bearing female subjects in future studies to identify sex-dependent differences in the response of the circadian system to HCC. It would also be of interest to detect the interaction between the development and progression of HCC and aging, which is correlated with dampened circadian rhythms, on the SCN function and the rhythmic behavior in further studies.

5. Conclusions

We propose a mechanism whereby cancer-related inflammation and/or neuroactive metabolites of liver dysfunction impair the circadian system at the level of the SCN. Our data suggest a double effect, on the one hand, with regard to neuronal activity and neuropeptides and, on the other hand, with regard to glial activity and oxidative stress. Both effects converge in a dysfunction of the molecular clockwork, which results in altered locomotor activity due to changed SCN rhythmic output. Our study contributes to the understanding of chronodisruption in cancer/liver diseases and could help develop corresponding therapeutic strategies to obtain better treatment outcomes and improve the quality of life of the patients.

Supplementary Materials: The following supporting information can be downloaded at: <https://www.mdpi.com/article/10.3390/biomedicines12102202/s1>, Figure S1. Liver inspection during autopsy; Figure S2. Anatomical localization of SCN and lateral hypothalamus (LH); Figure S3. Neuropeptides immunoreaction in SCN.

Author Contributions: Conceptualization, C.v.G., A.A.H.A. and H.-W.K.; methodology, M.Y., S.A.H., L.A.Y., F.F.A.P. and A.A.H.A.; validation, A.A.H.A.; formal analysis, M.Y. and A.A.H.A.; data curation, M.Y., L.A.Y., F.F.A.P. and A.A.H.A.; writing original draft preparation, M.Y. and A.A.H.A.; visualization, M.Y., L.A.Y., F.F.A.P. and A.A.H.A.; supervision, C.v.G.; project administration, C.v.G. and H.-W.K. All authors have read and agreed to the published version of the manuscript.

Funding: Soha A. Hassan is supported by the German Egyptian Research Long-term Scholarship (GERLS) Program of the German Academic Exchange Service (DAAD), Germany, and the Ministry of Higher Education and Scientific Research, Egypt (Fund ID: 57222240). This publication is supported by Heinrich Heine University, Düsseldorf, Germany.

Institutional Review Board Statement: Animal experiments were approved by the Regional Council Darmstadt and the North Rhine-Westphalia State Agency for Nature, Environment and Consumer Protection (LANUV), Germany (Reference number: AZ 81-02.04.2018-A146, date of approval: 12 June 2018) and conformed to federal guidelines and Directive 2010/63/EU of the European Union of Animal Care.

Informed Consent Statement: Not applicable.

Data Availability Statement: The dataset supporting the conclusions of this article is available upon reasonable request to the corresponding author without restriction.

Acknowledgments: The authors acknowledge Ralf Fassbender, Hanna Bellert, Angelika Hallenberger, and Ursula Lammersen for their excellent technical support.

Conflicts of Interest: The authors have no competing interests.

Abbreviations

AVP: arginine vasopressin, CRF: cancer-related fatigue, DAB: 3,3'-diaminobenzidine, GFAP: fibrillary acidic protein, HCC: Hepatocellular carcinoma, IR: immunoreaction, 8-OHdG: 8-hydroxydeoxyguanosine, PB: Phenobarbital, PBS: phosphate buffered saline, PVN: paraventricular nucleus of the hypothalamus, RHT: retino-hypothalamic tract, SCN: suprachiasmatic nucleus, SEM: standard error of the mean, VIP: vasoactive intestinal peptide, ZT: Zeitgeber Time.

References

- Swain, M.G.; Jones, D.E.J. Fatigue in chronic liver disease: New insights and therapeutic approaches. *Liver Int. Off. J. Int. Assoc. Study Liver* **2019**, *39*, 6–19. [\[CrossRef\]](#)
- Singal, A.G.; Kanwal, F.; Llovet, J.M. Global trends in hepatocellular carcinoma epidemiology: Implications for screening, prevention and therapy. *Nat. Rev. Clin. Oncol.* **2023**, *20*, 864–884. [\[CrossRef\]](#)
- Rao, A.; Rich, N.E.; Marrero, J.A.; Yopp, A.C.; Singal, A.G. Diagnostic and Therapeutic Delays in Patients With Hepatocellular Carcinoma. *J. Natl. Compr. Cancer Netw.* **2021**, *19*, 1063–1071. [\[CrossRef\]](#)
- Qiu, X.; Li, M.; Wu, L.; Xin, Y.; Mu, S.; Li, T.; Song, K. Severe Fatigue is an Important Factor in the Prognosis of Patients with Advanced Hepatocellular Carcinoma Treated with Sorafenib. *Cancer Manag. Res.* **2020**, *12*, 7983–7992. [\[CrossRef\]](#)
- Ee, C.; Kay, S.; Reynolds, A.; Lovato, N.; Lacey, J.; Koczwara, B. Lifestyle and integrative oncology interventions for cancer-related fatigue and sleep disturbances. *Maturitas* **2024**, *187*, 108056. [\[CrossRef\]](#)
- Sleight, A.G.; Crowder, S.L.; Skarbinski, J.; Coen, P.; Parker, N.H.; Hoogland, A.I.; Gonzalez, B.D.; Playdon, M.C.; Cole, S.; Ose, J.; et al. A New Approach to Understanding Cancer-Related Fatigue: Leveraging the 3P Model to Facilitate Risk Prediction and Clinical Care. *Cancers* **2022**, *14*, 1982. [\[CrossRef\]](#)
- Herzog, E.D.; Hermanstynne, T.; Smyllie, N.J.; Hastings, M.H. Regulating the Suprachiasmatic Nucleus (SCN) Circadian Clockwork: Interplay between Cell-Autonomous and Circuit-Level Mechanisms. *Cold Spring Harb. Perspect. Biol.* **2017**, *9*, a027706. [\[CrossRef\]](#)
- Silver, R.; Kriegsfeld, L.J. Circadian rhythms have broad implications for understanding brain and behavior. *Eur. J. Neurosci.* **2014**, *39*, 1866–1880. [\[CrossRef\]](#)
- Hastings, M.H.; Maywood, E.S.; Brancaccio, M. Generation of circadian rhythms in the suprachiasmatic nucleus. *Nat. Rev. Neurosci.* **2018**, *19*, 453–469. [\[CrossRef\]](#)
- Ono, D.; Honma, K.I.; Honma, S. Roles of Neuropeptides, VIP and AVP, in the Mammalian Central Circadian Clock. *Front. Neurosci.* **2021**, *15*, 650154.
- Morin, L.P. Neuroanatomy of the extended circadian rhythm system. *Exp. Neurol.* **2013**, *243*, 4–20. [\[CrossRef\]](#) [\[PubMed\]](#)
- Pfeffer, M.; Korf, H.W.; von Gall, C. Chronotype and stability of spontaneous locomotor activity rhythm in BMAL1-deficient mice. *Chronobiol. Int.* **2015**, *32*, 81–91. [\[CrossRef\]](#) [\[PubMed\]](#)
- Pfeffer, M.; Muller, C.M.; Mordel, J.; Meissl, H.; Ansari, N.; Deller, T.; Korf, H.W.; von Gall, C. The mammalian molecular clockwork controls rhythmic expression of its own input pathway components. *J. Neurosci.* **2009**, *29*, 6114–6123. [\[CrossRef\]](#)
- Brancaccio, M.; Edwards, M.D.; Patton, A.P.; Smyllie, N.J.; Chesham, J.E.; Maywood, E.S.; Hastings, M.H. Cell-autonomous clock of astrocytes drives circadian behavior in mammals. *Science* **2019**, *363*, 187–192. [\[CrossRef\]](#)

15. Ali, A.A.H.; Stahr, A.; Ingenwerth, M.; Theis, M.; Steinhäuser, C.; von Gall, C. Connexin30 and Connexin43 show a time-of-day dependent expression in the mouse suprachiasmatic nucleus and modulate rhythmic locomotor activity in the context of chronodisruption. *Cell Commun. Signal.* **2019**, *17*, 61. [[CrossRef](#)]
16. Mazuski, C.; Abel, J.H.; Chen, S.P.; Hermanstynne, T.O.; Jones, J.R.; Simon, T.; Doyle, F.J.; Herzog, E.D. Entrainment of Circadian Rhythms Depends on Firing Rates and Neuropeptide Release of VIP SCN Neurons. *Neuron* **2018**, *99*, 555–563.e555. [[CrossRef](#)]
17. Todd, W.D.; Venner, A.; Anaclet, C.; Broadhurst, R.Y.; De Luca, R.; Bandaru, S.S.; Issokson, L.; Hablitz, L.M.; Cravetchi, O.; Arrigoni, E.; et al. Suprachiasmatic VIP neurons are required for normal circadian rhythmicity and comprised of molecularly distinct subpopulations. *Nat. Commun.* **2020**, *11*, 4410. [[CrossRef](#)]
18. Jones, J.R.; Simon, T.; Lones, L.; Herzog, E.D. SCN VIP Neurons Are Essential for Normal Light-Mediated Resetting of the Circadian System. *J. Neurosci. Off. J. Soc. Neurosci.* **2018**, *38*, 7986–7995. [[CrossRef](#)] [[PubMed](#)]
19. Reghunandan, V. Vasopressin in circadian function of SCN. *J. Biosci.* **2020**, *45*, 140. [[CrossRef](#)]
20. Gau, D.; Lemberger, T.; von Gall, C.; Kretz, O.; Le Minh, N.; Gass, P.; Schmid, W.; Schibler, U.; Korf, H.W.; Schutz, G. Phosphorylation of CREB Ser142 regulates light-induced phase shifts of the circadian clock. *Neuron* **2002**, *34*, 245–253. [[CrossRef](#)]
21. Gall, C.v.; Duffield, G.E.; Hastings, M.H.; Kopp, M.D.A.; Dehghani, F.; Korf, H.-W.; Stehle, J.H. CREB in the Mouse SCN: A Molecular Interface Coding the Phase-Adjusting Stimuli Light, Glutamate, PACAP, and Melatonin for Clockwork Access. *J. Neurosci.* **1998**, *18*, 10389–10397. [[CrossRef](#)] [[PubMed](#)]
22. von Gall, C. The Effects of Light and the Circadian System on Rhythmic Brain Function. *Int. J. Mol. Sci.* **2022**, *23*, 2778. [[CrossRef](#)] [[PubMed](#)]
23. Matsubara, Y.; Kiyohara, H.; Teratani, T.; Mikami, Y.; Kanai, T. Organ and brain crosstalk: The liver-brain axis in gastrointestinal, liver, and pancreatic diseases. *Neuropharmacology* **2022**, *205*, 108915. [[CrossRef](#)]
24. Hunt, N.J.; Wahl, D.; Westwood, L.J.; Lockwood, G.P.; Le Couteur, D.G.; Cogger, V.C. Targeting the liver in dementia and cognitive impairment: Dietary macronutrients and diabetic therapeutics. *Adv. Drug Deliv. Rev.* **2022**, *190*, 114537. [[CrossRef](#)]
25. Görg, B.; Qvartskhava, N.; Bidmon, H.J.; Palomero-Gallagher, N.; Kircheis, G.; Zilles, K.; Häussinger, D. Oxidative stress markers in the brain of patients with cirrhosis and hepatic encephalopathy. *Hepatology* **2010**, *52*, 256–265. [[CrossRef](#)]
26. Haussinger, D.; Dhiman, R.K.; Felipo, V.; Gorg, B.; Jalan, R.; Kircheis, G.; Merli, M.; Montagnese, S.; Romero-Gomez, M.; Schnitzler, A.; et al. Hepatic encephalopathy. *Nat. Rev. Dis. Primers* **2022**, *8*, 43. [[CrossRef](#)]
27. Haussinger, D.; Butz, M.; Schnitzler, A.; Gorg, B. Pathomechanisms in hepatic encephalopathy. *Biol. Chem.* **2021**, *402*, 1087–1102. [[CrossRef](#)] [[PubMed](#)]
28. Schulien, I.; Hasselblatt, P. Diethylnitrosamine-induced liver tumorigenesis in mice. *Methods Cell Biol.* **2021**, *163*, 137–152. [[CrossRef](#)]
29. Wang, Z.; Wang, Y.; Huang, J.; Xu, J.; Chen, F.; Zhu, Z.; Gao, L.; Qin, J.; Liu, B.; Liang, C. Sleep Disturbance Affects Immune Factors in Clinical Liver Cancer Patients. *Curr. Oncol.* **2022**, *29*, 7943–7952. [[CrossRef](#)]
30. Huang, T.W.; Cheung, D.S.T.; Xu, X.; Loh, E.W.; Lai, J.H.; Su, W.W.; Wu, S.S.; Lin, C.C. Relationship Between Diurnal Cortisol Profile and Sleep Quality in Patients With Hepatocellular Carcinoma. *Biol. Res. Nurs.* **2020**, *22*, 139–147. [[CrossRef](#)]
31. Qu, M.; Zhang, G.; Qu, H.; Vu, A.; Wu, R.; Tsukamoto, H.; Jia, Z.; Huang, W.; Lenz, H.J.; Rich, J.N.; et al. Circadian regulator BMAL1::CLOCK promotes cell proliferation in hepatocellular carcinoma by controlling apoptosis and cell cycle. *Proc. Natl. Acad. Sci. USA* **2023**, *120*, e2214829120. [[CrossRef](#)] [[PubMed](#)]
32. Jiang, Y.; Shen, X.; Fasaie, M.B.; Zhi, F.; Chai, L.; Ou, Y.; Feng, H.; Liu, S.; Liu, Y.; Yang, S. The Expression and Function of Circadian Rhythm Genes in Hepatocellular Carcinoma. *Oxidative Med. Cell. Longev.* **2021**, *2021*, 4044606. [[CrossRef](#)]
33. Lin, Y.M.; Chang, J.H.; Yeh, K.T.; Yang, M.Y.; Liu, T.C.; Lin, S.F.; Su, W.W.; Chang, J.G. Disturbance of circadian gene expression in hepatocellular carcinoma. *Mol. Carcinog.* **2008**, *47*, 925–933. [[CrossRef](#)] [[PubMed](#)]
34. Yang, S.L.; Yu, C.; Jiang, J.X.; Liu, L.P.; Fang, X.; Wu, C. Hepatitis B virus X protein disrupts the balance of the expression of circadian rhythm genes in hepatocellular carcinoma. *Oncol. Lett.* **2014**, *8*, 2715–2720. [[CrossRef](#)]
35. Hassan, S.A.; Ali, A.A.H.; Sohn, D.; Flögel, U.; Jänicke, R.U.; Korf, H.W.; von Gall, C. Does timing matter in radiotherapy of hepatocellular carcinoma? An experimental study in mice. *Cancer Med.* **2021**, *10*, 7712–7725. [[CrossRef](#)]
36. Yassine, M.; Hassan, S.A.; Sommer, S.; Yücel, L.A.; Bellert, H.; Hallenberger, J.; Sohn, D.; Korf, H.W.; von Gall, C.; Ali, A.A.H. Radiotherapy of the Hepatocellular Carcinoma in Mice Has a Time-of-Day-Dependent Impact on the Mouse Hippocampus. *Cells* **2022**, *12*, 61. [[CrossRef](#)] [[PubMed](#)]
37. Hassan, S.A.; Ali, A.A.H.; Yassine, M.; Sohn, D.; Pfeffer, M.; Jänicke, R.U.; Korf, H.W.; von Gall, C. Relationship between locomotor activity rhythm and corticosterone levels during HCC development, progression, and treatment in a mouse model. *J. Pineal Res.* **2021**, *70*, e12724. [[CrossRef](#)]
38. Garofalo, S.; Coccozza, G.; Mormino, A.; Bernardini, G.; Russo, E.; Ielpo, D.; Andolina, D.; Ventura, R.; Martinello, K.; Renzi, M.; et al. Natural killer cells and innate lymphoid cells 1 tune anxiety-like behavior and memory in mice via interferon- γ and acetylcholine. *Nat. Commun.* **2023**, *14*, 3103. [[CrossRef](#)]
39. Suzuki, S.; Handa, R.J. Estrogen receptor-beta, but not estrogen receptor-alpha, is expressed in prolactin neurons of the female rat paraventricular and supraoptic nuclei: Comparison with other neuropeptides. *J. Comp. Neurol.* **2005**, *484*, 28–42. [[CrossRef](#)]
40. Peng, H.; Zhang, J.; Zhang, P.P.; Chen, L.; Tang, L.L.; Yang, X.J.; He, Q.M.; Wen, X.; Sun, Y.; Liu, N.; et al. ARNTL hypermethylation promotes tumorigenesis and inhibits cisplatin sensitivity by activating CDK5 transcription in nasopharyngeal carcinoma. *J. Exp. Clin. Cancer Res.* **2019**, *38*, 11. [[CrossRef](#)]

41. Imai, Y.; Iбата, I.; Ito, D.; Ohsawa, K.; Kohsaka, S. A novel gene *iba1* in the major histocompatibility complex class III region encoding an EF hand protein expressed in a monocytic lineage. *Biochem. Biophys. Res. Commun.* **1996**, *224*, 855–862. [[CrossRef](#)] [[PubMed](#)]
42. Pegram, C.N.; Eng, L.F.; Wikstrand, C.J.; McComb, R.D.; Lee, Y.L.; Bigner, D.D. Monoclonal antibodies reactive with epitopes restricted to glial fibrillary acidic proteins of several species. *Neurochem. Pathol.* **1985**, *3*, 119–138. [[CrossRef](#)] [[PubMed](#)]
43. Angeloni, C.; Malaguti, M.; Rizzo, B.; Barbalace, M.C.; Fabbri, D.; Hrelia, S. Neuroprotective effect of sulforaphane against methylglyoxal cytotoxicity. *Chem. Res. Toxicol.* **2015**, *28*, 1234–1245. [[CrossRef](#)]
44. Moreno-Paublete, R.; Canlon, B.; Cederroth, C.R. Differential Neural Responses Underlying the Inhibition of the Startle Response by Pre-Pulses or Gaps in Mice. *Front. Cell. Neurosci.* **2017**, *11*, 19. [[CrossRef](#)]
45. Öztürk, M.; Ingenwerth, M.; Sager, M.; von Gall, C.; Ali, A.A.H. Does a Red House Affect Rhythms in Mice with a Corrupted Circadian System? *Int. J. Mol. Sci.* **2021**, *22*, 2288. [[CrossRef](#)] [[PubMed](#)]
46. Franklin, K.B.J.; Paxinos, G. *Paxinos and Franklin's The Mouse Brain in Stereotaxic Coordinates*, 4th ed.; Academic Press: Amsterdam, The Netherlands, 2013.
47. Liddel, S.A.; Barres, B.A. Reactive Astrocytes: Production, Function, and Therapeutic Potential. *Immunity* **2017**, *46*, 957–967. [[CrossRef](#)]
48. Lier, J.; Streit, W.J.; Bechmann, I. Beyond Activation: Characterizing Microglial Functional Phenotypes. *Cells* **2021**, *10*, 2236. [[CrossRef](#)]
49. Mogavero, M.P.; DelRosso, L.M.; Fanfulla, F.; Bruni, O.; Ferri, R. Sleep disorders and cancer: State of the art and future perspectives. *Sleep. Med. Rev.* **2021**, *56*, 101409. [[CrossRef](#)]
50. Verma, D.; Hashim, O.; Jayapalan, J.; Subramanian, P. Effect of melatonin on antioxidant status and circadian activity rhythm during hepatocarcinogenesis in mice. *J. Cancer Res. Ther.* **2014**, *10*, 1040–1044.
51. Moody, T.W. Peptide receptors as cancer drug targets. *Ann. N. Y. Acad. Sci.* **2019**, *1455*, 141–148. [[CrossRef](#)]
52. Amidi, A.; Wu, L.M. Circadian disruption and cancer- and treatment-related symptoms. *Front. Oncol.* **2022**, *12*, 1009064. [[CrossRef](#)]
53. Costa, R.; Mangini, C.; Domenie, E.D.; Zarantonello, L.; Montagnese, S. Circadian rhythms and the liver. *Liver Int.* **2023**, *43*, 534–545. [[CrossRef](#)]
54. Fattovich, G.; Stroffolini, T.; Zagni, I.; Donato, F. Hepatocellular carcinoma in cirrhosis: Incidence and risk factors. *Gastroenterology* **2004**, *127*, S35–S50. [[CrossRef](#)]
55. Hamnett, R.; Chesham, J.E.; Maywood, E.S.; Hastings, M.H. The Cell-Autonomous Clock of VIP Receptor VPAC2 Cells Regulates Period and Coherence of Circadian Behavior. *J. Neurosci. Off. J. Soc. Neurosci.* **2021**, *41*, 502–512. [[CrossRef](#)]
56. Kahan, A.; Mahe, K.; Dutta, S.; Kassraian, P.; Wang, A.; Gradinaru, V. Immediate responses to ambient light in vivo reveal distinct subpopulations of suprachiasmatic VIP neurons. *iScience* **2023**, *26*, 107865. [[CrossRef](#)]
57. Collins, B.; Pierre-Ferrer, S.; Muheim, C.; Lukacsovich, D.; Cai, Y.; Spinnler, A.; Herrera, C.G.; Wen, S.; Winterer, J.; Belle, M.D.C.; et al. Circadian VIPergic Neurons of the Suprachiasmatic Nuclei Sculpt the Sleep-Wake Cycle. *Neuron* **2020**, *108*, 486–499.e5. [[CrossRef](#)]
58. Kalsbeek, A.; Buijs, R.M. Organization of the neuroendocrine and autonomic hypothalamic paraventricular nucleus. *Handb. Clin. Neurol.* **2021**, *180*, 45–63. [[CrossRef](#)]
59. Takahashi, Y.; Okamura, H.; Yanaiharu, N.; Hamada, S.; Fujita, S.; Iбата, Y. Vasoactive intestinal peptide immunoreactive neurons in the rat suprachiasmatic nucleus demonstrate diurnal variation. *Brain Res.* **1989**, *497*, 374–377. [[CrossRef](#)]
60. Bult, A.; van der Zee, E.A.; Compaan, J.C.; Lynch, C.B. Differences in the number of arginine-vasopressin-immunoreactive neurons exist in the suprachiasmatic nuclei of house mice selected for differences in nest-building behavior. *Brain Res.* **1992**, *578*, 335–338. [[CrossRef](#)]
61. Hofman, M.A. The human circadian clock and aging. *Chronobiol. Int.* **2000**, *17*, 245–259. [[CrossRef](#)]
62. Hara, M.; Takeba, Y.; Iiri, T.; Ohta, Y.; Ootaki, M.; Watanabe, M.; Watanabe, D.; Koizumi, S.; Otsubo, T.; Matsumoto, N. Vasoactive intestinal peptide increases apoptosis of hepatocellular carcinoma by inhibiting the cAMP/Bcl-xL pathway. *Cancer Sci.* **2018**, *110*, 235–244. [[CrossRef](#)]
63. Ravindranathan, S.; Passang, T.; Li, J.-M.; Wang, S.; Dhamsania, R.; Ware, M.B.; Zaidi, M.Y.; Zhu, J.; Cardenas, M.; Liu, Y.; et al. Targeting vasoactive intestinal peptide-mediated signaling enhances response to immune checkpoint therapy in pancreatic ductal adenocarcinoma. *Nat. Commun.* **2022**, *13*, 6418. [[CrossRef](#)]
64. Reubi, J.C.; Läderach, U.; Waser, B.; Gebbers, J.-O.; Robberecht, P.; Laissue, J.A. Vasoactive Intestinal Peptide/Pituitary Adenylate Cyclase-activating Peptide Receptor Subtypes in Human Tumors and Their Tissues of Origin. *Cancer Res.* **2000**, *60*, 3105–3112.
65. Moody, T.W.; Nucho-Berenguer, B.; Jensen, R.T. Vasoactive intestinal peptide/pituitary adenylate cyclase activating polypeptide, and their receptors and cancer. *Curr. Opin. Endocrinol. Diabetes Obes.* **2016**, *23*, 38–47. [[CrossRef](#)]
66. Su, Y.; van der Spek, R.; Foppen, E.; Kwakkel, J.; Fliers, E.; Kalsbeek, A. Effects of adrenalectomy on daily gene expression rhythms in the rat suprachiasmatic and paraventricular hypothalamic nuclei and in white adipose tissue. *Chronobiol. Int.* **2015**, *32*, 211–224. [[CrossRef](#)]
67. Oesch, L.T.; Adamantidis, A.R. Sleep and Metabolism: Implication of Lateral Hypothalamic Neurons. In *The Orexin System. Basic Science and Role in Sleep Pathology*; Steiner, M.A., Yanagisawa, M., Clozel, M., Eds.; S.Karger AG: Basel, Switzerland, 2021; Volume 45.

68. Aston-Jones, G.; Smith, R.J.; Sartor, G.C.; Moorman, D.E.; Massi, L.; Tahsili-Fahadan, P.; Richardson, K.A. Lateral hypothalamic orexin/hypocretin neurons: A role in reward-seeking and addiction. *Brain Res.* **2010**, *1314*, 74–90. [[CrossRef](#)]
69. Loh, D.H.; Dragich, J.M.; Kudo, T.; Schroeder, A.M.; Nakamura, T.J.; Waschek, J.A.; Block, G.D.; Colwell, C.S. Effects of vasoactive intestinal peptide genotype on circadian gene expression in the suprachiasmatic nucleus and peripheral organs. *J. Biol. Rhythm.* **2011**, *26*, 200–209. [[CrossRef](#)]
70. Brancaccio, M.; Maywood, E.S.; Chesham, J.E.; Loudon, A.S.; Hastings, M.H. A Gq-Ca²⁺ axis controls circuit-level encoding of circadian time in the suprachiasmatic nucleus. *Neuron* **2013**, *78*, 714–728. [[CrossRef](#)]
71. Vosko, A.; van Diepen, H.C.; Kuljis, D.; Chiu, A.M.; Heyer, D.; Terra, H.; Carpenter, E.; Michel, S.; Meijer, J.H.; Colwell, C.S. Role of vasoactive intestinal peptide in the light input to the circadian system. *Eur. J. Neurosci.* **2015**, *42*, 1839–1848. [[CrossRef](#)]
72. An, S.; Harang, R.; Meeker, K.; Granados-Fuentes, D.; Tsai, C.A.; Mazuski, C.; Kim, J.; Doyle, F.J., 3rd; Petzold, L.R.; Herzog, E.D. A neuropeptide speeds circadian entrainment by reducing intercellular synchrony. *Proc. Natl. Acad. Sci. USA* **2013**, *110*, E4355–E4361. [[CrossRef](#)]
73. Bunger, M.K.; Wilsbacher, L.D.; Moran, S.M.; Clendenin, C.; Radcliffe, L.A.; Hogenesch, J.B.; Simon, M.C.; Takahashi, J.S.; Bradfield, C.A. Mop3 is an essential component of the master circadian pacemaker in mammals. *Cell* **2000**, *103*, 1009–1017. [[CrossRef](#)] [[PubMed](#)]
74. von Gall, C.; Noton, E.; Lee, C.; Weaver, D.R. Light does not degrade the constitutively expressed BMAL1 protein in the mouse suprachiasmatic nucleus. *Eur. J. Neurosci.* **2003**, *18*, 125–133. [[CrossRef](#)] [[PubMed](#)]
75. Zuo, Y.; Hou, Y.; Wang, Y.; Yuan, L.; Cheng, L.; Zhang, T. Circadian misalignment impairs oligodendrocyte myelination via Bmal1 overexpression leading to anxiety and depression-like behaviors. *J. Pineal Res.* **2024**, *76*, e12935. [[CrossRef](#)] [[PubMed](#)]
76. Ikeda, M.; Ikeda, M. Bmal1 is an essential regulator for circadian cytosolic Ca²⁺ rhythms in suprachiasmatic nucleus neurons. *J. Neurosci. Off. J. Soc. Neurosci.* **2014**, *34*, 12029–12038. [[CrossRef](#)] [[PubMed](#)]
77. Barca-Mayo, O.; Pons-Espinal, M.; Follert, P.; Armirotti, A.; Berdondini, L.; De Pietri Tonelli, D. Astrocyte deletion of Bmal1 alters daily locomotor activity and cognitive functions via GABA signalling. *Nat. Commun.* **2017**, *8*, 14336. [[CrossRef](#)]
78. Patton, A.P.; Smyllie, N.J.; Chesham, J.E.; Hastings, M.H. Astrocytes Sustain Circadian Oscillation and Bidirectionally Determine Circadian Period, But Do Not Regulate Circadian Phase in the Suprachiasmatic Nucleus. *J. Neurosci.* **2022**, *42*, 5522–5537. [[CrossRef](#)]
79. Ali, A.A.H.; Schwarz-Herzke, B.; Rollenhagen, A.; Anstötz, M.; Holub, M.; Lübke, J.; Rose, C.R.; Schnittler, H.J.; von Gall, C. Bmal1-deficiency affects glial synaptic coverage of the hippocampal mossy fiber synapse and the actin cytoskeleton in astrocytes. *Glia* **2020**, *68*, 947–962. [[CrossRef](#)]
80. Lawrence, J.M.; Schardien, K.; Wigdahl, B.; Nonnemacher, M.R. Roles of neuropathology-associated reactive astrocytes: A systematic review. *Acta Neuropathol. Commun.* **2023**, *11*, 42. [[CrossRef](#)]
81. Matsui, F.; Yamaguchi, S.T.; Kobayashi, R.; Ito, S.; Nagashima, S.; Zhou, Z.; Norimoto, H. Ablation of microglia does not alter circadian rhythm of locomotor activity. *Mol. Brain* **2023**, *16*, 34. [[CrossRef](#)]
82. Honzlová, P.; Semenovykh, K.; Sumová, A. The Circadian Clock of Polarized Microglia and Its Interaction with Mouse Brain Oscillators. *Cell. Mol. Neurobiol.* **2023**, *43*, 1319–1333. [[CrossRef](#)]
83. Ito, D.; Imai, Y.; Ohsawa, K.; Nakajima, K.; Fukuuchi, Y.; Kohsaka, S. Microglia-specific localisation of a novel calcium binding protein, Iba1. *Brain Res. Mol. Brain Res.* **1998**, *57*, 1–9. [[CrossRef](#)]
84. Lawther, A.J.; Phillips, A.J.K.; Chung, N.C.; Chang, A.; Ziegler, A.I.; Debs, S.; Sloan, E.K.; Walker, A.K. Disrupting circadian rhythms promotes cancer-induced inflammation in mice. *Brain Behav. Immun. Health* **2022**, *21*, 100428. [[CrossRef](#)]
85. Gonzalo-Gobernado, R.; Reimers, D.; Herranz, A.S.; Díaz-Gil, J.J.; Osuna, C.; Asensio, M.J.; Baena, S.; Rodríguez-Serrano, M.; Bazán, E. Mobilization of neural stem cells and generation of new neurons in 6-OHDA-lesioned rats by intracerebroventricular infusion of liver growth factor. *J. Histochem. Cytochem. Off. J. Histochem. Soc.* **2009**, *57*, 491–502. [[CrossRef](#)]
86. Pekny, M.; Pekna, M. Astrocyte reactivity and reactive astrogliosis: Costs and benefits. *Physiol. Rev.* **2014**, *94*, 1077–1098. [[CrossRef](#)]
87. Jayakumar, A.R.; Norenberg, M.D. Endothelial-astrocytic interactions in acute liver failure. *Metab. Brain Dis.* **2013**, *28*, 183–186. [[CrossRef](#)]
88. Tilg, H.; Diehl, A.M. Cytokines in alcoholic and nonalcoholic steatohepatitis. *N. Engl. J. Med.* **2000**, *343*, 1467–1476. [[CrossRef](#)]
89. Li, H.; Tofigh, A.M.; Amirfakhraei, A.; Chen, X.; Tajik, M.; Xu, D.; Motevalli, S. Modulation of astrocyte activity and improvement of oxidative stress through blockage of NO/NMDAR pathway improve posttraumatic stress disorder (PTSD)-like behavior induced by social isolation stress. *Brain Behav.* **2022**, *12*, e2620. [[CrossRef](#)]
90. Chen, Y.; Qin, C.; Huang, J.; Tang, X.; Liu, C.; Huang, K.; Xu, J.; Guo, G.; Tong, A.; Zhou, L. The role of astrocytes in oxidative stress of central nervous system: A mixed blessing. *Cell Prolif.* **2020**, *53*, e12781. [[CrossRef](#)]
91. Iizumi, T.; Takahashi, S.; Mashima, K.; Minami, K.; Izawa, Y.; Abe, T.; Hishiki, T.; Suematsu, M.; Kajimura, M.; Suzuki, N. A possible role of microglia-derived nitric oxide by lipopolysaccharide in activation of astroglial pentose-phosphate pathway via the Keap1/Nrf2 system. *J. Neuroinflamm.* **2016**, *13*, 99. [[CrossRef](#)]
92. Valavanidis, A.; Vlachogianni, T.; Fiotakis, C. 8-hydroxy-2'-deoxyguanosine (8-OHdG): A critical biomarker of oxidative stress and carcinogenesis. *J. Environ. Sci. Health C Environ. Carcinog. Ecotoxicol. Rev.* **2009**, *27*, 120–139. [[CrossRef](#)]
93. Simicic, D.; Cudalbu, C.; Pierzchala, K. Overview of oxidative stress findings in hepatic encephalopathy: From cellular and ammonium-based animal models to human data. *Anal. Biochem.* **2022**, *654*, 114795. [[CrossRef](#)] [[PubMed](#)]

94. Rich, T.; Innominato, P.F.; Boerner, J.; Mormont, M.C.; Iacobelli, S.; Baron, B.; Jasmin, C.; Lévi, F. Elevated Serum Cytokines Correlated with Altered Behavior, Serum Cortisol Rhythm, and Dampened 24-Hour Rest-Activity Patterns in Patients with Metastatic Colorectal Cancer. *Clin. Cancer Res.* **2005**, *11*, 1757–1764. [[CrossRef](#)] [[PubMed](#)]
95. Crews, F.T.; Sarkar, D.K.; Qin, L.; Zou, J.; Boyadjieva, N.; Vetreno, R.P. Neuroimmune Function and the Consequences of Alcohol Exposure. *Alcohol. Res.* **2015**, *37*, 331–341, 344–351. [[PubMed](#)]
96. Padilla, J.; Osman, N.M.; Bissig-Choisat, B.; Grimm, S.L.; Qin, X.; Major, A.M.; Yang, L.; Lopez-Terrada, D.; Coarfa, C.; Li, F.; et al. Circadian dysfunction induces NAFLD-related human liver cancer in a mouse model. *J. Hepatol.* **2024**, *80*, 282–292. [[CrossRef](#)]
97. Kotsiliti, E. Understanding HCC sex disparities. *Nat. Rev. Gastroenterol. Hepatol.* **2022**, *19*, 147. [[CrossRef](#)]
98. Walton, J.C.; Bumgarner, J.R.; Nelson, R.J. Sex Differences in Circadian Rhythms. *Cold Spring Harb. Perspect. Biol.* **2022**, *14*, a039107. [[CrossRef](#)]

Disclaimer/Publisher’s Note: The statements, opinions and data contained in all publications are solely those of the individual author(s) and contributor(s) and not of MDPI and/or the editor(s). MDPI and/or the editor(s) disclaim responsibility for any injury to people or property resulting from any ideas, methods, instructions or products referred to in the content.